

University of Groningen

Bifurcation analysis of incompressible flow in a driven cavity

Wubs, F.W.; Tiesinga, G.; Veldman, A.E.P.

Published in:
EPRINTS-BOOK-TITLE

IMPORTANT NOTE: You are advised to consult the publisher's version (publisher's PDF) if you wish to cite from it. Please check the document version below.

Document Version
Publisher's PDF, also known as Version of record

Publication date:
2000

[Link to publication in University of Groningen/UMCG research database](#)

Citation for published version (APA):

Wubs, F. W., Tiesinga, G., & Veldman, A. E. P. (2000). Bifurcation analysis of incompressible flow in a driven cavity. In *EPRINTS-BOOK-TITLE* University of Groningen, Johann Bernoulli Institute for Mathematics and Computer Science.

Copyright

Other than for strictly personal use, it is not permitted to download or to forward/distribute the text or part of it without the consent of the author(s) and/or copyright holder(s), unless the work is under an open content license (like Creative Commons).

The publication may also be distributed here under the terms of Article 25fa of the Dutch Copyright Act, indicated by the "Taverne" license. More information can be found on the University of Groningen website: <https://www.rug.nl/library/open-access/self-archiving-pure/taverne-amendment>.

Take-down policy

If you believe that this document breaches copyright please contact us providing details, and we will remove access to the work immediately and investigate your claim.

Downloaded from the University of Groningen/UMCG research database (Pure): <http://www.rug.nl/research/portal>. For technical reasons the number of authors shown on this cover page is limited to 10 maximum.

Bifurcation analysis of incompressible flow in a driven cavity*

F.W. Wubs[†], G. Tiesinga[‡] and A.E.P. Veldman[§]

Abstract

Knowledge of the transition point of steady to periodic flow and the frequency occurring hereafter is becoming increasingly more important in engineering applications. By the Newton–Picard method — a method related to the recursive projection method — periodic solutions can be computed, which makes such knowledge available. In the paper this method is applied to study the bifurcation behavior of the flow in a driven cavity at Reynolds numbers between 7500 and 10000. For the time discretization the θ -method is used and for the space discretization a symmetry-preserving finite-volume method. The implicit relations occurring after linearization are solved by the multilevel ILU solver MRILU. Our results extend findings from earlier work with respect to the transition point.

Key words: Algebraic multilevel methods, ILU-factorization, eigenvalue problems, continuation, bifurcation.

AMS subject classifications: 65H17, 65F10, 65F15, 65M20, 76D05, 76E30.

1 Introduction

The paper discusses the application of the Newton–Picard method to study the transition from steady to (quasi)-periodic flow, as described by the incompressible Navier–Stokes equations. Such studies are not only interesting from a theoretical point of view, but they also have practical applications, e.g. in fluid-structure interaction problems.

The study has been performed for flow in a square lid-driven cavity. Cazemier *et al.* [2] have performed a similar study on a small (approximate) dynamical system resulting from a Galerkin discretization on a basis obtained by a proper orthogonal decomposition (or equivalently by a singular value decomposition) of snapshots of the flow on a very fine grid. The small system admits to compute the monodromy matrix, i.e. the amplification matrix for perturbations of the solution, the order of which is equal to the number of degrees of freedom in the system. The eigenvalues of the monodromy matrix determine whether a periodic solution is stable or not. In [2] it was observed that the behaviour of the small dynamical system predicted reasonably well the behaviour of the system on the very fine grid. In the present study we make use of the Newton–Picard method in which the monodromy matrix restricted to the space consisting of the most critical modes is constructed. This allows to study the bifurcation behaviour of the full Navier–Stokes system; this in contrast to the approximate system studied by Cazemier *et al.* [2].

The Newton–Picard method has been developed by Lust and Roose [5, 6] and implemented in the software tool PDECONT. In itself the Newton–Picard method is a generalization of the recursive projection method (RPM) of Shroff and Keller [8]. In PDECONT the PDE is solved by using an implicit method; we have implemented MRILU [1] for solving the occurring linearized systems.

With respect to the transition point we recall the following. Well known are the results of Ghia *et al.* from 1982 [3], who computed solutions up to a Reynolds number of 10000; they however found only stationary solutions. Poliashenko and Aidun [7] found a transition point at $Re = 7763 \pm 2\%$. This point has been confirmed by the accurate results of Cazemier *et al.* [2], who found transition at $Re = 7972$, with an emerging period of $T = 2.2$ seconds.

*This research has been supported by the Netherlands Organization for Scientific Research (N.W.O.)

[†]Research Institute for Mathematics and Computer Science, University of Groningen, P.O.Box 800, 9700 AV Groningen, Email: wubs@math.rug.nl; <http://www.math.rug.nl/~wubs>

[‡]Email: ena@math.rug.nl

[§]Email: veldman@math.rug.nl; <http://www.math.rug.nl/~veldman>

2 Discretization

In the method of lines a PDE is first discretized in space, which results in a large system of ODEs

$$\frac{dx}{dt} = f(x, \gamma), \quad t > 0, \quad x(0) = x_0.$$

Its bifurcation behaviour can be studied by a continuation method, such as PDECONT. The latter software tool requires from the user two subroutines: one for the right-hand side $f(x, \gamma)$ and one for the solution of the ODE starting with some x_0 integrated over a time period t with parameter γ . For the time integration the θ -method has been implemented. In the following we treat, in the spirit of the method-of-lines approach, the discretization in space and time separately.

2.1 Space-discretization

The space discretization is defined on a staggered non-uniform grid, for which various discretization choices are available. Experience has learned that a proper treatment of the convective terms is crucial for numerical stability and accuracy (see [9]).

The equations are discretized using a second-order symmetry-preserving finite-volume approach, which we will explain by considering the continuity equation and the momentum equation in one dimension (Figure 1). For the

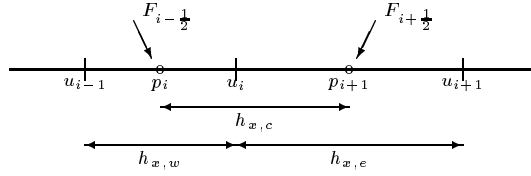


Figure 1: The one-dimensional control volume

continuity equation the standard grid cell is taken as a control volume, yielding for the cell around p_i

$$(1) \quad u_i - u_{i-1} = 0.$$

The momentum control volume is positioned around the point u_i . The discrete x -momentum equation becomes

$$h_{x,c} \frac{du_{i,j}}{dt} + (\hat{F}(u)_{i+\frac{1}{2}} - \hat{F}(u)_{i-\frac{1}{2}}) = -(p_{i+1} - p_i),$$

where $\hat{F}(u)_{i+\frac{1}{2}} = u_{i+\frac{1}{2}}u_{i+\frac{1}{2}} - \nu(u_{i+1} - u_i)/h_{x,e}$ is the discrete approximation of the convective and diffusive flux given by $F(u) = uu - \nu u_x$. For reasons that will become clear later, for the moment only the second factor $u_{i+\frac{1}{2}}$ will be replaced by the average of the surrounding values $u_{i+\frac{1}{2}} = (u_i + u_{i+1})/2$. In this way the discrete convective flux combination reads

$$(2) \quad \frac{1}{2}u_{i+\frac{1}{2}}(u_{i+1} + u_i) - \frac{1}{2}u_{i-\frac{1}{2}}(u_i + u_{i-1}) = \frac{1}{2}u_{i+\frac{1}{2}}u_{i+1} + \frac{1}{2}(u_{i+\frac{1}{2}} - u_{i-\frac{1}{2}})u_i - \frac{1}{2}u_{i-\frac{1}{2}}u_{i-1}.$$

Of each product in this expression, the first factor is considered as the coefficient and the second factor as the unknown.

The discretization in (2) has a property which is important for stability: the central term of the convective part in the momentum equations vanishes, which can be seen as follows. The central coefficient can be rewritten as (and only here we substitute $u_{i+\frac{1}{2}}$ once again)

$$\frac{1}{2}(u_{i+\frac{1}{2}} - u_{i-\frac{1}{2}}) = \frac{1}{4}(u_{i+1} + u_i) - \frac{1}{4}(u_i + u_{i-1}) = \frac{1}{4}(u_{i+1} - u_i) + \frac{1}{4}(u_i - u_{i-1}) = 0.$$

Note that the coefficient, apart from a factor, becomes precisely the sum of the continuity equations (1) around p_i and p_{i+1} , and hence the final step in the above derivation produces zero! In this way we have established in the discrete form (2) a similar action which is always possible in the continuous form: rewriting the convective term in the momentum equations to skew-symmetric form by using the continuity equation. This is easily extended to higher dimensions. Numerically this property implies that in a pure convective problem discrete energy is conserved exactly: the convective terms cannot give rise to artificial blow up or dissipation; see [9] for more details.

2.2 Time discretization

For the time discretization the θ -method is used, given by

$$x_{n+1} = x_n + \Delta t f((1 - \theta)x_n + \theta x_{n+1}).$$

For $\theta = 1/2$ and $\theta = 1$ this is the implicit midpoint and backward Euler method, respectively. As initial guess for the solution the extrapolation formula $x_{n+1} = 2x_n - x_{n-1}$ is used. The implicit relations are solved by the Newton method and the occurring linear equations are solved by MRILU. The Newton–Picard method computes perturbations from a steady state; these perturbations are so small that one factorization per time period is enough.

The choice of θ in the application is delicate. Consider for a moment that we are studying the stability of a steady state by perturbing the solution. Then the choice $\theta = 1/2$ gives an amplification of magnitude almost one for high-frequency components, though in reality these are highly damped. The choice $\theta = 1$ will give excessive damping in the problem, e.g. eigenvalues with a relative large imaginary part and a small positive real part may still have an amplification with magnitude less than 1 though they would be unstable if the ODE would be integrated exactly. We will make the material more precise.

Suppose we want to study the effect of perturbations of a steady state over a time period T with n equal time steps, hence $\Delta t = T/n$. Then for each eigenvalue λ of the Jacobian matrix of f we have the following amplification r

$$(3) \quad r = [(1 + (1 - \theta)\lambda\Delta t)/(1 - \theta\lambda\Delta t)]^n.$$

In the Newton–Picard process the perturbations corresponding to the most dominant r 's, say all r 's which are in magnitude larger than 0.95, will be computed. We want that this dominant subspace contains the same perturbations as those dominating in the time-continuous case. So we try to find θ close to $1/2$, such that for $\lambda\Delta t$ large the magnitudes of the corresponding r 's are less than those corresponding to $\lambda\Delta t$ close to the imaginary axes. For large $\lambda\Delta t$ (3) leads to the approximation

$$|r| \approx [(1 - \theta)/\theta]^n \approx \exp[-4(\theta - 1/2)n],$$

whereas for small $\lambda\Delta t$

$$r \approx \exp(\lambda T) \exp[2 \frac{\theta - 1/2}{n} (\lambda T)^2],$$

which shows more clearly how (3) depends on θ and n . Using an estimate of the important eigenvalues which are of the order of magnitude $\lambda T \approx 2\pi i$ one can get an idea of choosing θ and n (or Δt). In our case we used θ 's ranging from 0.51 to 0.502.

3 PDECONT and the Newton–Picard method

In this section the Newton–Picard method, which is at the basis of PDECONT, will be described in short. The underlying idea of the method can already be found in [4, 8], where it is applied to steady computations.

$$(4) \quad x = g(x).$$

One may think here of a steady state computation by means of a time integration method over some period, or of detecting a periodic solution of a PDE. The solution space is split in two orthogonal subspaces \mathcal{P} and \mathcal{P}^\perp with projectors P and Q , respectively. Let $p_0 = Px_0$ and $q_0 = Qx_0$, then we iterate according to

$$(5) \quad p_{i+1} = p_i + C_1(Pg(x_i) - p_i),$$

$$(6) \quad q_{i+1} = q_i + C_2(Qg(x_i) - q_i),$$

$$(7) \quad x_{i+1} = p_{i+1} + q_{i+1}.$$

Here C_1 and C_2 should be chosen such that good convergence is obtained in both subspaces. In the paper of Shroff and Keller [8] C_2 is just the identity matrix, yielding a Picard iteration in \mathcal{P}^\perp , and C_1 is minus the inverse of the Jacobian of $Pg(x_i) - p_i$:

$$C_1 = - \frac{\partial(Pg(p_i + q_i) - p_i)}{\partial p_i}.$$

This makes the Jacobian of the right-hand side of the p -update equation zero and results in a Newton step in \mathcal{P} . Let the columns of V be the orthogonal vectors spanning \mathcal{P} , then every $p \in \mathcal{P}$ can be written as $p = V\hat{p}$. Herewith the p -update equation (5) can be rewritten as

$$\hat{p}_{i+1} = \hat{p}_i + (I - V^T g_x V)^{-1} (V^T g(V\hat{p}_i + q_i) - \hat{p}_i).$$

In the periodic case the matrix $V^T g_x V$ is an approximation of the monodromy matrix restricted to \mathcal{P} . The directional derivatives $g_x V_i$, where V_i is the i -th column of V , can be found by numerical differentiation

$$(8) \quad g_x(x_n)V_i = (g(x_n + \varepsilon V_i) - g(x_n))/\varepsilon.$$

The projections P and Q can be written in terms of V : $P = VV^T$ and $Q = I - P = I - VV^T$. In the actual computation one works with \hat{p} and q .

We are left with the problem of finding V . Its columns build the invariant subspace \mathcal{P} which usually is the space corresponding to the dominant eigenvalues of g_x . V can be found in a variety of ways. Here it is found by accelerated orthogonal iteration, which is a generalization of the power method. The matrix involved is g_x which is not available in explicit form, but we can compute g_x times a vector by numerical differentiation as shown in (8). For every vector this entails the integration over one period. This added to the fact that orthogonal iteration is slowly converging when the magnitude of the eigenvalues cluster, it is not surprising that the detection of V takes most of the execution time of the method (a number of hours for one iteration in our case).

Note that the presented iteration is in general more contractive than the original fixed point problem (4). Even if the fixed point problem is mildly unstable, with only a few eigenvalues of g_x in magnitude larger than one, then RPM is converging if the eigenvectors corresponding to those eigenvalues are in \mathcal{P} .

4 Numerical results

The method has been used to test the stability for both steady state and periodic problems; both types of results will be presented below. All computations are on a non-uniform 128×128 grid.

4.1 Along the steady solution branch

As a starting solution for the Newton–Picard process the steady-state solution at $\text{Re} = 7500$ has been used. The time step Δt was set at 0.125 seconds and $\theta = 0.51$. The time step is adapted by the program such that its multiple fits in the period (which is artificial in this steady case and initialized at 1.5 seconds). For the Newton method a stopping criterion of 10^{-12} is imposed on the correction (max norm). This is needed to reduce the numerical error in the numerical differentiation, which is important for achieving sufficient convergence.

For the construction of an invariant subspace 22 vectors were found to suffice in the orthogonal iteration. The vectors which meet the stopping criterion and have a corresponding Floquet multiplier greater than 0.95 are used for the invariant subspace \mathcal{P} .

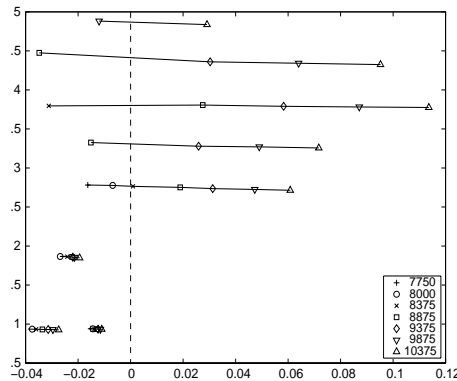


Figure 2: Eigenvalues in the complex plane for various Reynolds numbers. Values with positive real part correspond with unstable modes.

A plot of the eigenvalues is given in Fig. 2. These eigenvalues are computed from the inverse of (3), hence the eigenvalues are independent of θ . The first bifurcation occurs in the neighbourhood of $\text{Re} = 8375$ with $\text{Im}(\lambda) = 2.76$, hence a time period of 2.28. The difference with Cazemier's value 7972 is due to the fact that we have applied a coarser grid (to save on computing time), but the solution has the same period. Next to this one, four other Hopf bifurcations were encountered below $\text{Re} = 10000$.

4.2 Along periodic solution branches

If we want to compute the periodic solution then we have to consider the transition of the time integration process instead of looking where the eigenvalues of the Jacobian pass the imaginary axis. This may shift the transition point. In order to minimize this effect we increased the accuracy of the time integration by using $\theta = 0.502$ and $\Delta t = 0.06125$. The computation was restarted at $\text{Re} = 8000$ and steps 100 were used in the continuation. The search space for the invariant subspace was extended to 30 vectors. It was observed that the steady solution became unstable at $\text{Re} = 8400$ as before, for a perturbation with a period of about 2.3 seconds.

Continuation along the periodic branch was started at $\text{Re} = 8550$ using the steady solution plus half the first vector in the basis. At $\text{Re} = 9150$ this solution becomes unstable. The period of the frequency of this unstable mode is about 1.43 (or $\text{Im}(\lambda) = 4.40$), again computed by the inverse of (3) which holds approximately now. The corresponding eigenvalue 4.40 is also present in Fig. 2. From $\text{Re} = 9250$ upward increments of 250 were taken until 10000; no new unstable modes were found.

The movement of the Floquet multipliers in the complex plane is shown in the left-hand plot of Fig. 3. The marks in this plot make it possible to follow what happens when the Reynolds number increases: they follow the sequence $\circ, \times, +, *, \square, \diamond$. All occurring multipliers can be traced back to the components given in Fig. 2. The radius of the Floquet multipliers is scaled in order to stretch the plot near the unit circle. On the dash-dotted and dashed line the radius is 0.90 and 0.95, respectively.

For a further branch the computation was started at $\text{Re} = 8700$ using the steady solution plus half the vector corresponding to the component causing the second Hopf bifurcation. The Reynolds number was increased by 100. The result is displayed in the middle plot of Fig. 3. Since we start here from the second bifurcation from the steady state, the steady state is unstable and so is the periodic solution. However, almost immediately the unstable perturbation becomes stable and the eigenvalue is driven away from the unit circle. The periodic solution remains stable for the remainder of the computation to $\text{Re} = 10000$.

The right-hand plot in Fig. 3 shows a partial bifurcation diagram from the results computed here; it gives a qualitative behaviour of the system. When the stationary solution becomes unstable at $\text{Re} \approx 8375$ a periodic branch emerges; this periodic branch is stable up to $\text{Re} \approx 9150$. At $\text{Re} \approx 8600$ a second unstable periodic solution emerges from the steady state. This periodic solution restabilizes at $\text{Re} \approx 8800$. It is observed that in the range $\text{Re} = 8800$ to 9150 two stable periodic solutions exist. From the unstable stationary solution other periodic solutions emerge at Reynolds numbers of about 9000, 9100 and 10000, respectively. These solutions are (initially) unstable.

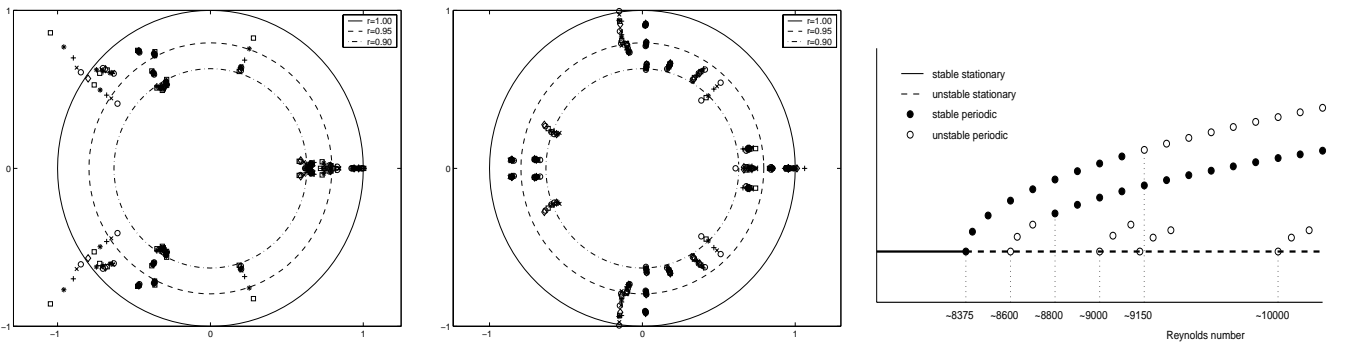


Figure 3: Floquet multipliers of the periodic solution emerging at the first (left) and second (middle) Hopf bifurcation and a bifurcation diagram (right). The radius of the Floquet multipliers is scaled with $100r^{-1}$

5 Conclusions

Large-scale bifurcation analysis of periodic solutions by computational means is possible. However the current version of PDECONT consumes a lot of computer time, which is due to the slow convergence of the invariant subspace. The use of implicit time integration is made possible through the availability of good iterative solvers, such as CG-type methods preconditioned by MRILU. Special care has to be taken that only the Floquet multipliers of interest are found. The convective space discretization should be chosen such that it does not interfere with the stability of the flow.

For the driven-cavity flow a complicated bifurcation pattern has been found, with (at least) five Hopf bifurcations for Reynolds numbers below 10000. Also, along some of the periodic solution branches additional bifurcation points have been identified. These findings confirm and extend earlier computations by Cazemier *et al.* [2].

References

- [1] E.F.F. Botta and F.W. Wubs. Matrix Renumbering ILU: An effective algebraic multilevel ILU-preconditioner for sparse matrices. *SIAM J. Matrix Anal. Appl.*, 20(4):1007–1026, 1999.
- [2] W. Cazemier, R.W.C.P. Verstappen, and A.E.P. Veldman. POD and low-dimensional models for driven cavity flows. *Physics of Fluids*, 10:1685–1699, 1998.
- [3] U. Ghia, K.N. Ghia, and C.T. Shin. High-Re solutions for incompressible flow using the Navier-Stokes equations and a multigrid method. *J. Comput. Phys.*, 48:387–411, 1982.
- [4] H. Jarausch and W. Mackens. Solving large nonlinear systems of equations by an adaptive condensation process. *Numer. Math.*, 50(6):633–653, 1987.
- [5] K. Lust. *Numerical bifurcation analysis of periodic solutions of partial differential equations*. PhD thesis, K.U. Leuven, Leuven, Belgium, 1997.
- [6] K. Lust and D. Roose. Computation and bifurcation analysis of periodic solutions of large-scale systems. In E. Doedel and L.S. Tuckerman, editors, *Numerical Methods for Bifurcation Problems and Large-Scale Dynamical Systems*, volume 119 of *Volumes in Mathematics and its Applications*. 2000.
- [7] M. Poliashenko and C.K. Aidun. A direct method for computation of simple bifurcations. *J. Comput. Phys.*, 121:246–260, 1995.
- [8] G. Shroff and H.B. Keller. Stabilization of unstable procedures: the recursive projection method. *SIAM J. Numer. Anal.*, 30(4):1099–1120, 1993.
- [9] R.W.C.P. Verstappen and A.E.P. Veldman. Spectro-consistent discretization of Navier-Stokes: a challenge to RANS and LES. *J. Engrg. Math.*, 34:163–179, 1998.